Asian Journal of Chemistry; Vol. 34, No. 12 (2022), 3231-3242

ASIAN JOURNAL OF CHEMISTRY

https://doi.org/10.14233/ajchem.2022.24042

Synthesis of Carboxamides and Carbothioamides of Phthalimide: Molecular Modeling and Biological Investigation

RENU GAVADIA, JYOTI RASGANIA and KOMAL JAKHAR*

Department of Chemistry, Maharshi Dayanand University, Rohtak-124001, India

*Corresponding author: E-mail: komal.jakhar@rediffmail.com

Received: 15 September 2022; *Accepted*: 3 October 2022; *Published online*: 25 November 2022; AJC-21049

A series of carboxamide and carbothioamide derivatives of phthalimide have been synthesized efficiently by employing water as a green reaction media. The synthesized *N*-substituted phthalimide derivatives have been characterized by spectroscopic, elemental and their quantum parameters, including molecular orbital energies are deduced by DFT modeling. The molecular docking of synthesized derivatives against B-DNA (pdb:1bna) displays favourable binding interactions and satisfactory docking scores, predicting their significant antimicrobial efficacy. The synthesized phthalimide derivatives were screened for *in vitro* antimicrobial and antioxidant activity using broth microdilution method and DPPH radical scavenging assay, respectively. Some of the title compounds exhibited promising the antimicrobial and antioxidant potential. The pharmacokinetics parameters and bioavailability of the title compounds were accessed by *in silico* ADMET analysis to envisage their drug efficacy.

Keywords: Phthalimide, Urea, Molecular docking, Antimicrobial, Antioxidant, ADMET analysis.

INTRODUCTION

Phthalimide is a versatile bicyclic imide having extensive applications in therapeutic sciences [1]. The distinct bioactive potential of phthalimide is associated with its unique structural features [2]. The presence of a hydrophobic aryl ring in phthalimide ensures its optimum lipophilicity, better permeability across biological membranes and higher bioavailability. Since the NH center of phthalimide is flanked between two carbonyl groups, phthalimide is acidic in nature, exhibits good solubility in polar media, forms salts with strong bases and can be arylated/alkylated. The hydrogen bonding potential of the imide group increases the binding capacity of phthalimide derivatives with different receptors and enzymes, which enhances their docking profile and therapeutic efficacy. Several *N*-substituted phthalimide derivatives were identified with promising pharmacological actions such as analgesic [3], antitumor [4], anti-inflammatory [5], anticonvulsant [6], antibacterial [5], antifungal [7], antimycobacterial [8], anti-hyperlipidemic [9], antimalarial [10], antioxidant [5], anti-angiogenic [11] and acetylcholinesterase inhibition [12], *etc*.

Urea and thiourea are privileged molecules in medicinal sciences and play a key role in the preparation of numerous biologically active compounds [13,14]. Urea and thiourea derivatives possess important applications in research laboratories, agricultural sciences, automobiles, corrosion inhibition and industries. Several optical, sensor and catalytic materials are identified with urea/thiourea scaffolds as main structural motifs [15]. A broad range of pharmacological properties are associated with urea and thiourea derivatives such as anticancer [16], antituberculosis [17], antimicrobial [18], antioxidant [19], antidiabetic [20], anticonvulsant [21], antiviral [22] and insecticidal [23], *etc.*

N-Substituted phthalimides are generally synthesized by thermal condensation of phthalic anhydride with different amine motifs. Several handling difficulties are associated with the traditional method, such as spontaneous decomposition of phthalic anhydride to phthalic acid, gaseous nature of lower aliphatic amines and spontaneous oxidation of aromatic amines during storage [24]. Therefore, the direct use of phthalimide for the preparation of its *N*-substituted derivatives is highly appreciable in terms of time and energy. On reaction with potassium hydroxide, phthalimide forms water-soluble salt called potassium phthalimide, which is a potent nucleophilic reagent extensively used in Gabriel phthalimide synthesis of

primary amines. Potassium phthalate can be easily prepared and used to synthesize desired structural motifs [25].

The design and synthesis of efficient therapeutic molecules are essential for pharmacological innovations. The distinct pharmacological competencies of phthalimide and (thio)ureas encouraged us to explore the preparation of their condensed derivative. To the best of our knowledge, direct condensation of potassium phthalimide with different (thio)urea scaffolds have not been reported in any synthetic study to date. This report presents an efficient synthesis of carboxamide and carbothioamide derivatives of phthalimide. The environmentally benign synthesis of organic compounds recommends the minimum use of hazardous organic solvents as they are highly volatile, flammable and carcinogenic [26]. Therefore, water as a reaction media is explored in this condensation as it is a natural, clean, non-flammable and non-toxic solvent and facilitates countless biological reactions. The selective heating power of microwaves is also explored for the preparation of title compounds as microwave-assisted reactions are identified with higher yields, reduced reaction times and increased selectivity [27]. The synthesized molecules have been screened for their *in vitro* antimicrobial and antioxidant activities.

Due to rapid technological advancements in medicinal sciences, in-advance screening of anticipated drug molecules is possible through docking and ADMET analysis to ascertain their therapeutic efficacies and drug likeliness. Several antibacterial compounds containing phthalimide as a pharmacophoric group exhibited effective DNA binding capabilities [28]. In present report, the DNA receptor was selected as a target in docking analysis with the synthesized phthalimide derivatives.

EXPERIMENTAL

All chemicals used were of synthetic grade, purchased from Sigma-Aldrich and used without further purification. Analytical thin-layer chromatographic glass plates precoated with silica gel G were used to examine the progress of the reaction. Melting points were measured in open capillaries using a paraffin wax bath and are uncorrected. A CEM microwave synthesizer Model no. 908010, with maximum power of 700W was utilized for microwave-assisted synthesis. CHN analyses were recorded on a Thermo Scientific (Flash 2000) CHN elemental analyzer. For recording IR, NMR and mass spectra of compounds, Nicolet iS50 FT-IR spectrometer, Bruker Advance Neo 500 MHz Spectrometer and XEVO G2-XS QTOF-Mass Spectrometer were used, respectively. For DFT modeling of synthesized molecules, the program module Avogadro and Orca [29,30] were utilized and correlation function B3LYP along with basis set def2-TZV(P) were used as the Orca parameters. A series of the carboxamide and carbothioamide derivatives of phthalimide were synthesized as outlined in **Scheme-I**.

General procedure for the synthesis of 1,3-dioxoisoindoline-2-carboxamides/carbothioamides (4a-j):

Method A: An equimolar mixture of potassium phthalimide and urea/thiourea substrate **(3a-j)** was dissolved in minimum amount of water and refluxed. The progress of the reaction was monitored with TLC (benzene:ethylacetate/2:8) and the reaction showed completion in 35-50 min depending upon the type of urea/thiourea substrate used. The excess solvent was evaporated and the crude solid product thus obtained was washed with a minimum amount of ice cold water, air dried and recrystallized with ethanol.

Method B: An equimolar mixture of potassium phthalimide and urea/thiourea substrate (**3a-j**) was mixed in a loosely stoppered 10 mL conical flask and homogenized with a few drops of water. The reaction mixture was exposed to microwave irradiation at 90 ºC and 180 W. The reaction showed a completion in 1-3 min depending upon the type of urea/thiourea substrate taken. Similar work-up procedure as explained in method A gives the title compounds in substantial yields.

1,3-Dioxoisoindoline-2-carboxamide (4a): White solid; m.p.: 225 ºC; Yield: 86% (reflux), 95% (MWI); R_f value: 0.79 (benzene:ethylacetate/2:8); m.w.: 190.16; IR (KBr, ν_{max}, cm^{-1}): 3300, 3230 (s, N-H), 3090 (s, C-H_{Ar}), 1760, 1751 (m, C=O_{imide}), 1680 (m, C=O_{amide}), 1538 (m, N-H_{bend}), 1290 (m, C-N); ^{1}H NMR (500 MHz, DMSO): δ 7.94-7.89 (m, 4H, Ar-H), 6.08 (s, 2H, NH_2); ^{13}C NMR (500 MHz, DMSO): δ 169.11 (C_d), 155.03 (C_e), 132.60 ($C_{a,c}$), 123.70 (C_b); HR-MS (*m/z*): 190.01 (72%), 174.28 (100%), 146.27, 104.17, 76.40, 69.47, 50.49, 44.84;

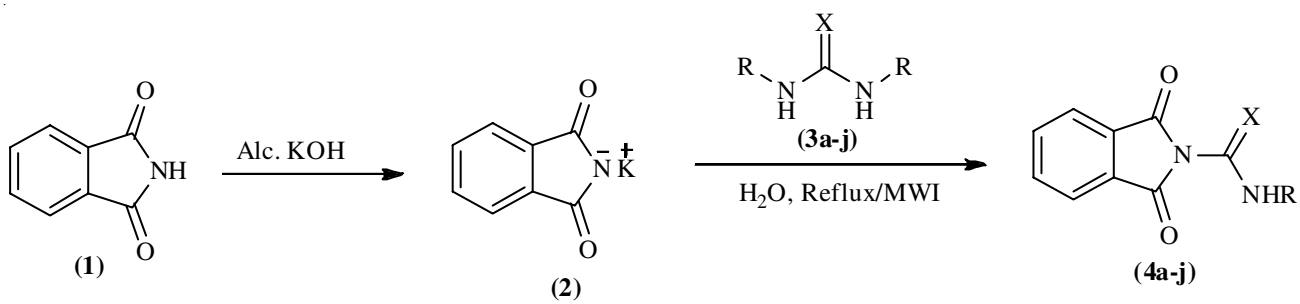

4a: X = O, R = H
4b: X = O, R = CH_3
4c: X = O, R = C_2H_5
4d: X = O, R = C_4H_9
4e: X = O, R = C_6H_{11}
4f: X = S, R = H
4g: X = S, R = CH_3
4h: X = S, R = C_2H_5
4i: X = S, R = C_4H_9
4j: X = S, R = C_6H_{11}

Scheme-I: Synthesis of carboxamide and carbothioamide derivatives of phthalimide

Elemental analysis calcd. (found) % of $C_9H_6N_2O_3$: C, 56.85 (56.76); H, 3.18 (3.13); N, 14.73 (17.62); O, 25.24 (25.18).

***N*-Methyl-1,3-dioxoisoindoline-2-carboxamide (4b):** White solid; m.p.: 200 ºC; Yield: 82% (reflux), 92% (MWI); R_f value: 0.89 (benzene:ethylacetate/2:8); m.w.: 204.18; IR (KBr, ν_{max}, cm^{-1}): 3305 (s, N-H), 3030 (m, C-H_{Ar}), 1770, 1745 (s, C=O_{imide}), 1660 (m, C=O_{amide}), 1520 (m, N-H_{bend}), 1257 (m, C-N); ^{1}H NMR (500 MHz, DMSO): δ 7.84-7.79 (m, 4H, Ar-H), 6.18 (s, 1H, NH), 2.90 (s, 3H, CH_3); ^{13}C NMR (500 MHz, DMSO): δ 170.24 (C_d), 156.62 (C_e), 133.00 ($C_{a,c}$), 124.46 (C_b), 26.42 (C_f); HR-MS (*m/z*): 204.09 (68%), 174.52 (100%), 146.19, 104.89, 76.92, 69.50, 58.19, 50.32; Elemental analysis calcd. (found) % of $C_{10}H_8N_2O_3$: C, 58.82 (58.75); H, 3.95 (3.83); N, 13.72 (13.60); O, 23.51 (23.40).

***N*-Ethyl-1,3-dioxoisoindoline-2-carboxamide (4c):** White solid; m.p.: 220 ºC; Yield: 81% (reflux), 92% (MWI); R_f value: 0.78 (benzene:ethylacetate/2:8); m.w.: 218.21; IR (KBr, ν_{max}, cm^{-1}): 3330 (s, N-H), 3085 (s, C-H_{Ar}), 1785, 1760 (s, C=O_{imide}), 1695 (m, C=O_{amide}), 1590 (m, N-H_{bend}), 1240 (m, C-N); ^{1}H NMR (500 MHz, DMSO): δ 7.68-7.65 (m, 4H, Ar-H), 6.20 (s, 1H, NH), 3.22 (q, 2H, CH_2), 1.16 (t, 3H, CH_3); ^{13}C NMR (500 MHz, DMSO): δ 169.60 (C_d), 154.66 (C_e), 131.56 ($C_{a,c}$), 123.49 (C_b), 34.24 (C_f), 16.02 (C_g); HR-MS (*m/z*): 218.29 (67%), 174.22 (100%), 146.49, 104.19, 76.02, 72.42, 69.80, 50.52; Elemental analysis calcd. (found) % of $C_{11}H_{10}N_2O_3$: C, 60.55 (60.43); H, 4.62 (4.54); N, 12.84 (12.78); O, 22.00 (22.09).

***N*-Butyl-1,3-dioxoisoindoline-2-carboxamide (4d):** White solid; m.p.: 90 ºC; Yield: 80% (reflux), 89% (MWI); R_f value: 0.87 (benzene:ethylacetate/2:8); m.w.: 246.26; IR (KBr, ν_{max}, cm^{-1}): 3350 (s, N-H), 3080 (s, C-H_{Ar}), 2990 (m, C-H_{alkyl}), 1730, 1710 (s, C=O_{imide}), 1680 (s, C=O_{amide}), 1510 (s, N-H_{bend}), 1205 (s, C-N); ^{1}H NMR (500 MHz, DMSO): δ 7.67-7.62 (m, 4H, Ar-H), 6.11 (s, 1H, NH), 2.94 (t, 2H, CH_2), 1.34-1.23 (m, 4H, CH_2), 0.86 (t, 3H, CH_3); ^{13}C NMR (500 MHz, DMSO): δ 168.11 (C_d), 155.58 (C_e), 130.57 ($C_{a,c}$), 122.37 (C_b), 40.95 (C_f), 31.45(C_g), 19.48 (C_h), 13.20 (C_i); HR-MS (*m/z*): 246.29 (48%), 174.32 (100%), 146.09, 104.59, 100.54, 76.72, 72.22, 69.60, 50.37; Elemental analysis calcd. (found) % of $C_{13}H_{14}N_2O_3$: C, 63.40 (63.34); H, 5.73 (5.65); N, 11.38 (11.24); O, 19.49 (19.38).

***N*-Cyclohexyl-1,3-dioxoisoindoline-2-carboxamide (4e):** White solid; m.p.: 191 ºC; Yield: 80% (reflux), 90% (MWI); R_f value: 0.39 (benzene:ethylacetate/2:8); m.w.: 272.30; IR (KBr, ν_{max}, cm^{-1}): 3390 (s, N-H), 3090 (s, C-H_{Ar}), 2985 (m, C-H_{Alkyl}), 1740, 1705 (s, C=O_{imide}), 1685 (m, C=O_{amide}), 1520 (m, N-H_{bend}), 1248 (m, C-N); ^{1}H NMR (500 MHz, DMSO): δ 7.82-7.78 (m, 4H, Ar-H), 5.97 (s, 1H, NH), 3.50-3.49 (m, 1H, $CH_{cyclohexyl}$), 1.73-1.15 (m, 10H, $CH_{cyclohexyl}$); ^{13}C NMR (500 MHz, DMSO): δ 169.46 (C_d), 153.61 (C_e), 132.44 ($C_{a,c}$), 121.43 (C_b), 52.73 (C_f), 32.23 (C_g), 25.63 (C_i), 24.58 (C_h); HR-MS (*m/z*): 272.07 (63%), 174.02 (100%), 146.69, 126.19, 104.83, 98.42, 76.22, 69.55, 50.39; Elemental analysis calcd. (found) % of $C_{15}H_{16}N_2O_3$: C, 66.16 (66.10); H, 5.92 (5.85); N, 10.29 (10.21); O, 17.63 (17.60).

1,3-Dioxoisoindoline-2-carbothioamide (4f): White solid; m.p.: 136 ºC; Yield: 86% (reflux), 95% (MWI); R_f value: 0.56 (benzene:ethylacetate/2:8); m.w.: 206.22; IR (KBr, ν_{max}, cm^{-1}): 3360, 3205 (s, N-H), 3010 (s, C-H_{Ar}), 1730, 1705 (s, C=O_{imide}), 1680 (m, C=O_{amide}), 1538 (s, N-H_{bend}), 1245 (m, C-N); ^{1}H NMR (500 MHz, DMSO): δ 7.84-7.80 (m, 4H, Ar-H), 7.13 (s, 2H, NH_2); ^{13}C NMR (500 MHz, DMSO): δ 178.25 (C_e), 171.22 (C_d), 134.61 ($C_{a,c}$), 123.36 (C_b); HR-MS (*m/z*): 206.29 (68%), 190.29 (100%), 146.09, 104.33, 76.92, 69.93, 60.06, 50.32; Elemental analysis calcd. (found) % of $C_9H_6N_2O_2S$: C, 52.42 (52.34); H, 2.93 (2.83); N, 13.58 (13.52); O, 15.52 (15.46); S, 15.55 (15.45).

***N*-Methyl-1,3-dioxoisoindoline-2-carbothioamide (4g):** White solid; m.p.: 120 ºC; Yield: 82% (reflux), 92% (MWI); R_f value: 0.59 (benzene:ethylacetate/2:8); m.w.: 220.25; IR (KBr, ν_{max}, cm^{-1}): 3350 (s, N-H), 3080 (s, C-H_{Ar}), 1765, 1705 (s, C=O_{imide}), 1695 (s, C=O_{amide}), 1550 (m, N-H_{bend}), 1246 (s, C-N); ^{1}H NMR (500 MHz, DMSO): δ 7.85-7.80 (m, 4H, Ar-H), 7.21 (s, 1H, NH), 2.98 (s, 3H, CH_3); ^{13}C NMR (500 MHz, DMSO): δ 179.26 (C_e), 172.25 (C_d), 134.44 ($C_{a,c}$), 121.51 (C_b), 30.23 (C_f); HR-MS (*m/z*): 220.26 (53%), 190.71 (100%), 146.77, 104.47, 76.04, 74.92, 69.44, 50.57; Elemental analysis calcd. (found) % of $C_{10}H_8N_2O_2S$: C, 54.53 (54.45); H, 3.66 (3.58); N, 12.72 (12.69); O, 14.53 (14.45); S, 14.56 (14.60).

***N*-Ethyl-1,3-dioxoisoindoline-2-carbothioamide (4h):** White solid; m.p.: 129 ºC; Yield: 83% (reflux), 91% (MWI); R_f value: 0.67 (benzene:ethylacetate/2:8); Mol. wt = 234.27; IR (KBr, ν_{max}, cm^{-1}): 3330 (s, N-H), 3020 (s, C-H_{Ar}), 1755, 1730 (s, C=O_{imide}), 1685 (s, C=O_{amide}), 1525 (m, N-H_{bend}), 1202 (m, C-N); ^{1}H NMR (500 MHz, DMSO): δ 7.72-7.69 (m, 4H, Ar-H), 7.00 (s, 1H, NH), 4.32 (q, 2H, CH_2), 1.21 (t, 3H, CH_3); ^{13}C NMR (500 MHz, DMSO): δ 178.27 (C_e), 170.23 (C_d), 133.29 ($C_{a,c}$), 122.53 (C_b), 41.49 (C_f), 15.63 (C_g); HR-MS (*m/z*): 234.23 (56%), 190.24 (100%), 146.02, 104.29, 88.42, 76.20, 69.60, 50.54, 44.92; Elemental analysis calcd. (found) % of $C_{11}H_{10}N_2O_2S$: C, 56.39 (56.30); H, 4.30 (4.33); N, 11.96 (11.82); O, 13.66 (13.59); S, 13.69 (13.55).

***N*-Butyl-1,3-dioxoisoindoline-2-carbothioamide (4i):** White solid; m.p.: 85 ºC; Yield: 80% (reflux), 90% (MWI); R_f value: 0.63 (benzene:ethylacetate/2:8); m.w.: 262.33;); IR (KBr, ν_{max}, cm^{-1}): 3323 (s, N-H), 3095 (s, C-H_{Ar}), 2920 (s, C-H_{alkyl}), 1745, 1702 (s, C=O_{imide}), 1630 (s, C=O_{amide}), 1565 (s, N-H_{bend}), 1304 (s, C-N); ^{1}H NMR (500 MHz, DMSO): δ 7.85-7.81 (m, 4H, Ar-H), 7.15 (s, 1H, NH), 3.11 (t, 2H, CH_2), 1.30-1.24 (m, 4H, CH_2), 0.87 (t, 3H, CH_3); ^{13}C NMR (500 MHz, DMSO): δ 177.56 (C_e), 169.27 (C_d), 132.34 ($C_{a,c}$), 122.51 (C_b), 44.45 (C_f), 31.45 (C_g), 19.98 (C_h), 13.23 (Ci) HR-MS (*m/z*): 262.29 (59%), 190.23 (100%), 146.55, 116.52, 104.63, 76.22, 72.52, 69.03, 50.12; Elemental analysis calcd. (found) % of $C_{13}H_{14}N_2O_2S$: C, 59.52 (59.48); H, 5.38 (5.29); N, 10.68 (10.62); O, 12.20 (12.10); S, 12.22 (12.15).

***N*-Cyclohexyl-1,3-dioxoisoindoline-2-carbothioamide (4j):** White solid; m.p.: 125 ºC; Yield: 80% (reflux), 88% (MWI); R_f value: 0.37 (benzene:ethylacetate/2:8); m.w.: 288.36; IR (KBr, ν_{max}, cm^{-1}): 3350 (s, N-H), 3030 (s, C-H_{Ar}), 2920 (m, C-H_{alkyl}), 1748, 1707 (s, C=O_{imide}), 1685 (m, C=O_{amide}), 1520 (s, N-H_{bend}), 1210 (m, C-N); ^{1}H NMR (500 MHz, DMSO): δ 7.85-7.82 (m, 4H, Ar-H), 6.92 (s, 1H, NH), 3.41-3.39 (m, 1H, $CH_{cyclohexyl}$), 1.73-1.14 (m, 10H, $CH_{cyclohexyl}$); ^{13}C NMR (500 MHz, DMSO): δ 177.44 (C_e), 171.61 (C_d), 133.43 ($C_{a,c}$), 121.42 (C_b), 58.78

(C_f), 32.25 (C_g), 27.73 (C_i), 25.58 (C_h); HR-MS (*m/z*): 288.43 (31%), 190.59 (100%), 146.33, 142.31, 104.84, 98.42, 83.14, 76.32, 69.58, 50.31; Elemental analysis calcd. (found) % of $C_{15}H_{16}N_2O_2S$: C, 62.48 (62.38); H, 5.59 (5.60); N, 9.71 (9.60); O, 11.10 (11.03); S, 11.12 (11.05).

Antimicrobial assay: The *in vitro* antimicrobial susceptibility of the synthesized compounds was explored using the resazurin based broth microdilution method [31]. The bacterial strains chosen were *Bacillus subtilis*, *Staphylococcus aureus*, *Escherichia coli* and *Salmonella typhi*. Ampicillin was used as a standard antibacterial drug. A stock solution of 2 mg/mL sample solution was prepared for the assay. The culture was maintained in nutrient broth obtained from Himedia at optimum temperature. A 50 µL of broth was added to each well of the 96-well microtiter plate, followed by the addition of sample solution with two-fold serial dilution in columns 2-10. The nutrient broth as a sterility control was added to the last column. A 20 µL of bacterial culture was added to each well of the plate. The microbial strains are allowed to grow for an incubation period of 12-16 h at 32 ºC. A 30 µL of 0.015% resazurin dye was added to each well, followed by an incubation period of another 2 h at 37 ºC. The MIC values of the synthesized phthalimide derivatives against bacterial strains were evaluated based on colour visualization of wells. A pink colour in a microtiter well indicates the growth of the microbial strains while blue indicates their inhibition.

Antifungal activity of all the synthesized compounds was determined against *Aspergillus niger* and *Rhizopus oryzae*. Fluconazole was used as a standard drug. A similar procedure was employed for antifungal assay using potato dextrose broth (PDB) as culture media and 72 h as incubation period. The MIC values of the title compounds against fungal strains were determined in a similar manner by addition of resazurin dye.

Antioxidant assay: The synthesized phthalimide derivative were screened for their antioxidant efficacy by DPPH assay [32] by measuring their free radical scavenging activity against commonly used stable free radical 2,2-diphenyl-1-picrylhyrazyl (DPPH) using ascorbic acid as a positive control. The free radicals of DPPH show a deep purple colour with strong absorbance at 517 nm as its characteristic indication of stability. Due to the pairing of the radicals either by electron or by hydrogen atom of the examined antioxidant compound, the purple colour of DPPH solution turns yellow, indicating the neutralization of DPPH free radical and is accounted as the antioxidant potency of that compound. Alternatively, a decrease in absorbance at 517 nm was regarded as the antioxidant activity of tested compound. In brief, a 1 mL aliquot of prepared concentrations (20, 40, 60, 80, 100 µg/mL) of the synthesized derivatives (**4a-j**) in methanol was added to 1 mL of freshly prepared 0.004% DPPH solution and the resultant solution is left for 0.5 h in a dark container. The absorbance was recorded at 517 nm and radical scavenging activity was determined as follows:

$$\text{Radical scavenging } (\%) = \frac{\text{Abs}_{\text{control}} - \text{Abs}_{\text{sample}}}{\text{Abs}_{\text{control}}} \times 100$$

Molecular docking: The DNA binding potential of the synthesized phthalimide derivatives in terms of binding energies and different interaction modes was explored by molecular docking studies. The 3D structure of B-DNA (pdb:1bna) was retrieved from protein data bank and fully optimized chemical structure of title compounds in pdb format were obtained by Avogadro program. Autodock Vina 4.2.1 was used for the protein preparation by deleting water molecules, followed by addition of polar hydrogen atoms and assigning appropriate charges [33]. The blind grid mapping was applied around the prepared DNA receptor and Discovery Studio Visualizer v21.1.0.20298 [34] was used to interpret the generated results in the form of 2D and 3D visualization of the recorded interactions together with their corresponding bond distances between chosen receptor and examined molecules.

ADMET analysis and toxicity assessment: Online available tool Swiss ADME [35] was utilized to evaluate the ADMET-related physiochemical and pharmacokinetic parameters of the synthesized phthalimide derivatives. Osiris Property Explorer [36] was utilized for real-time toxicity risk assessment in terms of mutagenic, tumerogenic, irritant and reproductive risks. Tricolour code with green, orange and red indications declares the drug candidates as safer, with moderate risk and at high risk, respectively.

RESULTS AND DISCUSSION

One step integration of diverse (thio)urea scaffolds with phthalimide was explored in the present report. Potassium phthalimide was synthesized according to the reported literature method [25]. The proposed structure of the synthesized compound was confirmed by spectroscopic and elemental analysis. Ammonia or other alkyl amine generated as a side product during the reaction is either a gaseous or liquid product that can be easily separated from the main product by evaporation or washing and recrystallization.

Two broad bands at 3300 and 3230 cm^{-1} and a peak at 1538 cm^{-1} in IR spectra of the synthesized compounds correspond to the stretching and bending vibration of the NH_2 group. The presence of two intense peaks at 1760 and 1751 cm^{-1} reveals the asymmetric and symmetric stretching vibrations of imide carbonyls, while a peak at 1680 cm^{-1} was identified for the stretching vibrations of the amide carbonyl group. A peak corresponding to C-N stretching was also recorded at 1290 cm^{-1}. In proton NMR, aromatic phthalimide protons were identified between δ 7.94-7.89 ppm resonating as multiple. A singlet at δ 6.08 ppm was recorded for the amide protons, while no peak was detected in the region of δ 10-12 ppm for the NH proton of phthalimide moiety, which confirms the completion of the reaction and formation of the desired phthalimide derivative. In ^{13}C NMR spectra, the presence of two characteristic peaks at δ 169.11 and 155.03 ppm corresponds to carbonyls of phthalimide ring and amide groups, respectively, further confirming proposed structure of the title compound. The molecular mass and fragmentation pattern of the synthesized compound was confirmed by its mass spectra.

The microwave-assisted synthesis of 1,3-dioxoisoindoline-2-carboxamide was also explored in anticipation of better yield and reduced reaction times. In an optimized procedure, an equimolar mixture of potassium phthalimide and urea was

homogenized with a few drops of water and exposed to microwave irradiation at 90 ºC and 180 W. The reaction showed completion in 1 min, as confirmed by TLC. A similar workup procedure gives the desired compound in 95% yield. Diverse carboxamide and carbothioamide substituted phthalimides were prepared following similar procedures.

HOMO-LUMO analysis: The calculated thermodynamic parameters of the synthesized phthalimide derivatives which provide an insight into their stability and reactivity are illustrated in Table-1. Compound **4a** has the highest stability among all the examined compounds, while compound **4h** has the highest reactivity with a lowest energy gap. The HOMO and LUMO for the representative compounds **4a** and **4h** with their respective energy gaps are illustrated in Fig. 1.

Antimicrobial activity: The antimicrobial activity of the synthesized carboxamide and carbothioamide derivatives of phthalimide are summarized in Table-2, which indicates that all the synthesized compounds exhibit promising antibacterial potential showing good to moderate activity. Compounds **4a** and **4b** were identified as the best antibacterial agent, while compounds **4e** and **4j** were completely inactive against both the fungal strains, other shows slight antifungal activity.

Antioxidant activity: The calculated IC_{50} value is an excellent parameter to ascertain the radical scavenging effect. It represents the typical concentration of examined compound required to scavenge half of the existing radicals. The evaluated % scavenging activity and IC_{50} for the synthesized compounds

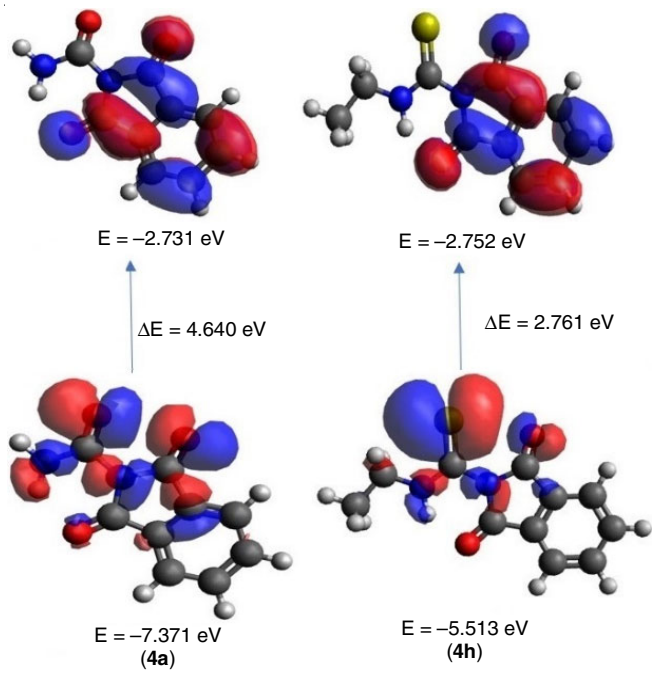

Fig. 1. HOMO and LUMO with energy gap for the compounds **4a** and **4h**

are summarized in Table-3. All the compounds possess remarkable antioxidant efficacy with good to moderate antiradical potential (61.08-74.86% at 100 µg/mL) and IC_{50} (59.65-81.15 µg/mL) in comparison to ascorbic acid. Compounds **4a** and

TABLE-1
THEORETICALLY CALCULATED QUANTUM PARAMETERS OF THE TITLE COMPOUNDS (**4a-j**)

Compd.	HOMO (eV)	LUMO (eV)	ΔE (eV)	Ionization potential (I)	Electron affinity (A)	Electro negativity (χ)	Hardness (η)	Softness (σ)	Chemical potential (μ)	Electro-phillicity (ω)
4a	-7.371	-2.731	4.640	7.371	2.731	5.051	2.320	0.215	-5.051	5.498
4b	-7.195	-2.681	4.514	7.195	2.681	4.938	2.257	0.221	-4.938	5.401
4c	-7.137	-2.656	4.481	7.137	2.656	4.896	2.240	0.223	-4.896	5.350
4d	-7.109	-2.642	4.467	7.109	2.642	4.875	2.233	0.223	-4.875	5.320
4e	-6.976	-2.626	4.350	6.976	2.626	4.801	2.175	0.229	-4.801	5.298
4f	-5.678	-2.843	2.835	5.678	2.843	4.260	1.417	0.352	-4.260	6.402
4g	-5.564	-2.777	2.787	5.564	2.777	4.170	1.393	0.358	-4.170	6.240
4h	-5.513	-2.752	2.761	5.513	2.752	4.132	1.380	0.362	-4.132	6.184
4i	-5.821	-2.687	3.134	5.821	2.687	4.254	1.567	0.319	-4.254	5.774
4j	-5.796	-2.635	3.161	5.796	2.635	4.215	1.580	0.316	-4.215	5.621

TABLE-2
ANTIMICROBIAL ACTIVITY IN MIC OF THE TITLE COMPOUNDS (**4a-j**) AND REFERENCE DRUGS IN mg/mL

Compd.	*E. coli*	*S. typhi*	*B. subtils*	*S. aureus*	*A. niger*	*R. oryzae*
4a	0.0625	0.0625	0.125	0.250	0.500	0.250
4b	0.0625	0.0625	0.125	0.250	0.500	0.250
4c	0.0625	0.0625	0.250	0.250	0.500	0.500
4d	0.0625	0.125	0.250	0.500	–	0.250
4e	0.125	0.0625	0.125	0.125	–	–
4f	0.0625	0.0625	0.500	0.250	0.250	0.125
4g	0.125	0.0625	0.500	0.250	0.250	0.125
4h	0.125	0.250	0.250	0.500	0.500	0.500
4i	0.125	0.250	0.250	0.500	–	0.500
4j	0.125	0.125	0.250	0.500	–	–
Ampicillin	0.03125	0.0625	0.125	0.0625	–	–
Fluconazole	–	–	–	–	0.0625	0.250

TABLE-3
PERCENTAGE RADICAL SCAVENGING AT DIFFERENT CONCENTRATIONS AND IC_{50} VALUES OF SYNTHESIZED PHTHALIMIDE DERIVATIVES EXPRESSED IN µg/mL

Compd.	Scavenging effect (%)					IC_{50} (µg/mL)
	20 µg/mL	40 µg/mL	60 µg/mL	80 µg/mL	100 µg/mL	
4a	35.66	42.13	49.58	58.13	65.16	59.65
4b	30.56	39.41	48.27	55.86	62.59	66.62
4c	13.02	29.16	45.61	59.74	71.52	68.39
4d	29.56	36.59	47.61	51.28	63.54	70.36
4e	29.68	37.22	46.37	54.13	66.41	67.16
4f	29.56	35.24	46.95	58.22	74.86	61.82
4g	20.16	31.25	46.85	57.23	71.76	67.04
4h	32.56	37.74	43.28	52.13	64.32	70.23
4i	18.29	26.57	37.12	49.55	61.08	81.15
4j	25.16	31.55	39.64	51.23	64.39	75.50
AA	29.63	46.18	65.23	75.15	90.12	44.98

4f exhibited the best IC_{50} values (59.65 and 61.82 µg/mL, respectively) among all the synthesized derivatives.

Molecular docking: The docking results revealed that all the derivatives have excellent binding potential with the DNA receptor. The binding efficiency can be attributed to the negative value of the binding energies. The best binding energy accounted in the investigation was -8.4 kcal/mol with RMSD value 0.00 for compound **4e**, which makes four hydrogen bonds with receptor DNA. The results of the docking studies including binding energies and name of the different residues making hydrogen bond with their respective bond distances are compiled in Table-4. The 3D and 2D interaction diagrams for all the compounds are compiled in Fig. 2. Since, the DNA interaction capacity can be identified as the drug efficacy of the synthesized compounds, the docking results can be further explored for developing DNA targeting therapeutic leads.

TABLE-4
DOCKING RESULTS WITH BINDING ENERGIES AND INTERACTIONS WITH RESPECTIVE DISTANCES (Å) FOR THE SYNTHESIZED COMPOUNDS (**4a-j**)

Compd.	B.E. (kcal/mol)	Residues making H-bond	Distance (Å)	Other interactions	Distance (Å)
4a	-6.8	DG A:10, DG B:16, DC B: 15, DC B: 15	2.01, 4.98, 2.84, 3.05	DG A: 12, DC A: 11	3.48, 3.77
4b	-7.1	DG B: 16, DG A: 10, DG B: 16, DG A: 10	5.16, 2.65, 2.22, 1.96	-	-
4c	-7.1	DG B: 16, DG A: 10, DG B: 16, DG A: 10	5.16, 1.96 2.21, 2.26	-	-
4d	-7.2	DG B: 16, DG A: 10	4.52, 2.20	DG A: 12, DA B:17, DG B:16	3.47, 5.20, 2.08
4e	-8.4	DG A: 10, DG A: 10, DG B: 16, DG B: 16	1.91, 2.87, 2.42, 2.39	DA B: 17	3.53
4f	-6.2	DG B: 16, DG A: 12, DG A: 10, DC A: 11	5.14, 2.94, 1.98, 1.96	DC A:11, DG B:14, DG A: 12	3.82, 2.34, 3.44
4g	-6.7	DG B: 16, DG A: 10, DC A: 11	5.01, 2.03, 2.39	-	-
4h	-6.4	DA B: 17, DG B: 16, DG A: 10	2.31, 2.14, 5.04	DA B: 18	5.15
4i	-6.5	DG A: 4, DA A:5, DG B: 22	6.97, 4.48, 3.61	DG B: 22, DC B: 23	6.06, 5.72
4j	-7.4	DG A: 10, DG B: 16	2.28, 4.48	-	-

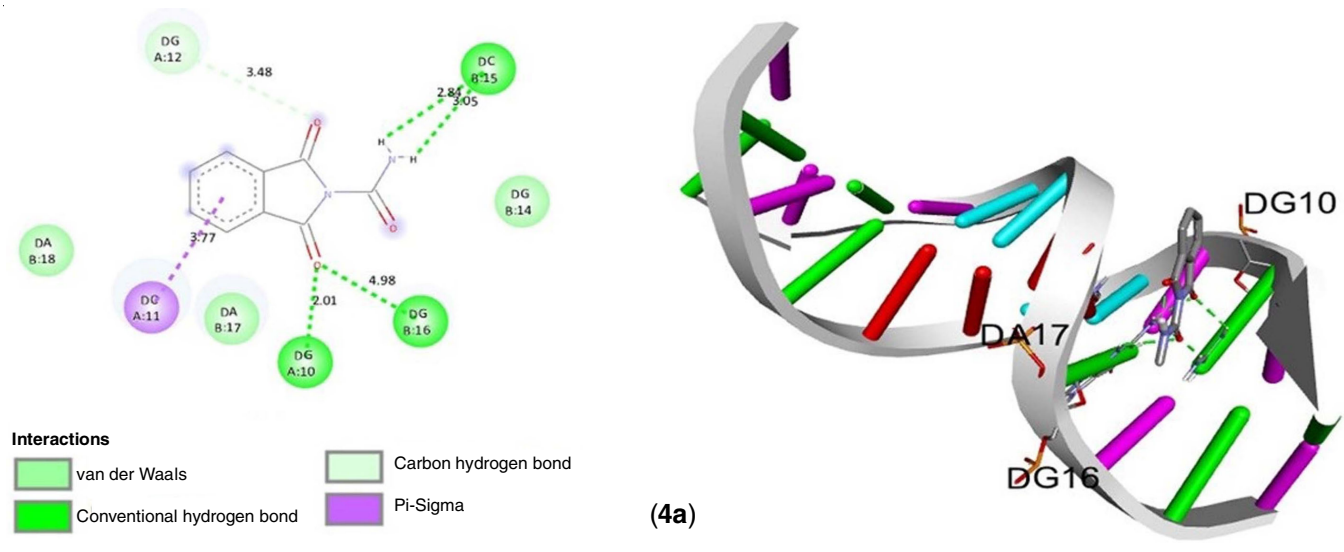

(**4a**)

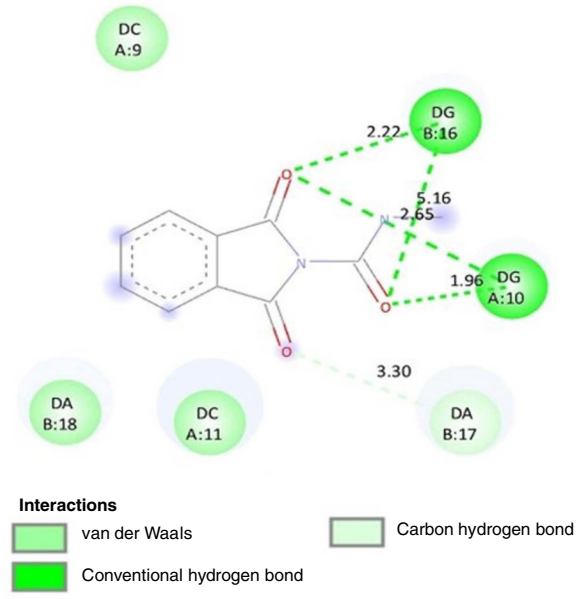
DC A:9
DG B:16
2.22
5.16
2.65
1.96
DG A:10
3.30
DA B:18
DC A:11
DA B:17
Interactions
van der Waals
Carbon hydrogen bond
Conventional hydrogen bond

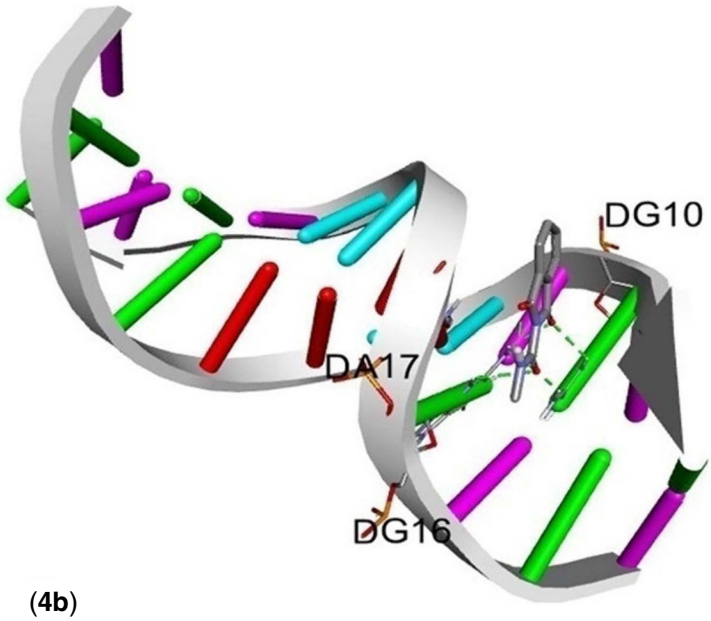
DG10
DA17
DG16

(**4b**)

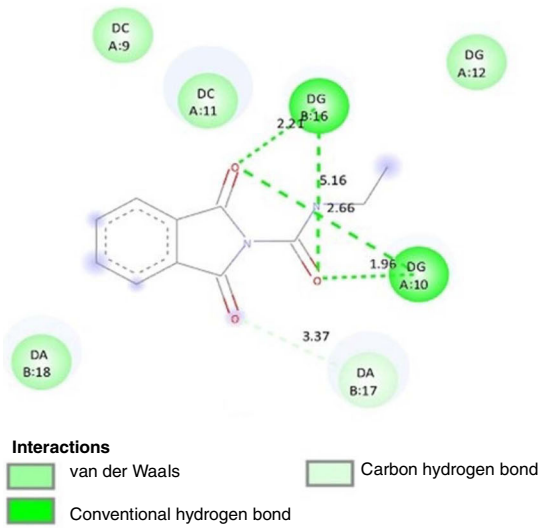
DC A:9
DG A:12
DC A:11
DG B:16
2.22
5.16
2.66
1.96
DG A:10
3.37
DA B:18
DA B:17
Interactions
van der Waals
Carbon hydrogen bond
Conventional hydrogen bond

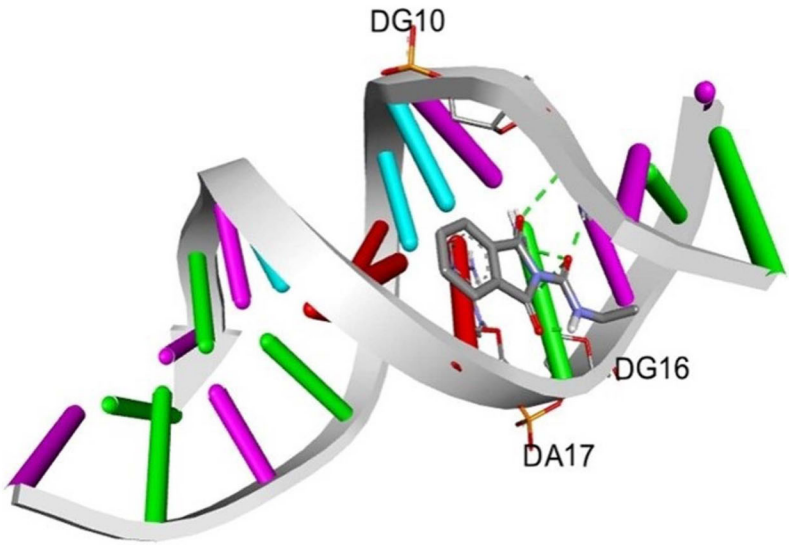
DG10
DG16
DA17

(**4c**)

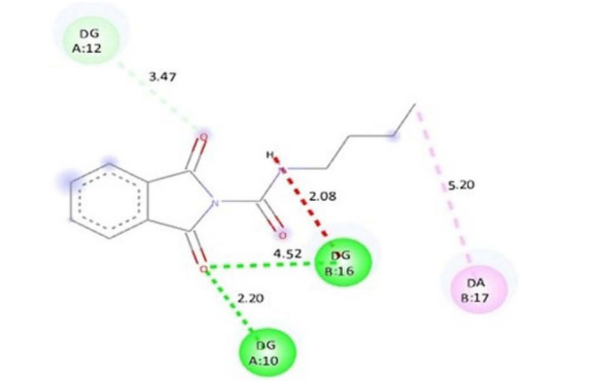
DG A:12
3.47
2.08
5.20
4.52
DG B:16
DA B:17
2.20
DG A:10
Interactions
Conventional hydrogen bond
Unfavorable donor-donor
Carbon hydrogen bond
Pi-Alkyl

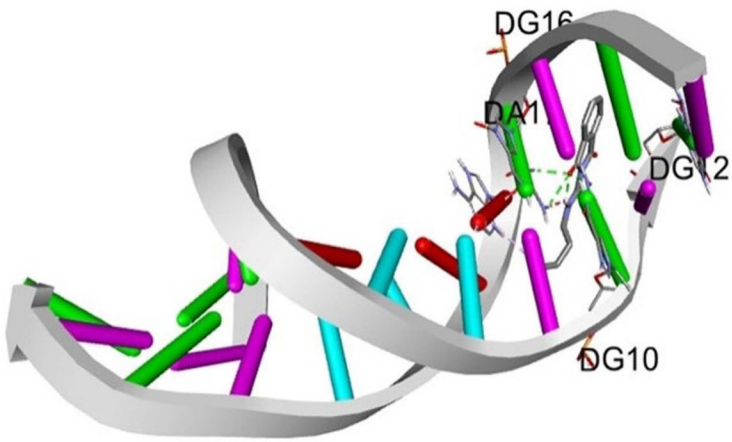
DG16
DA1
DG12
DG10

(**4d**)

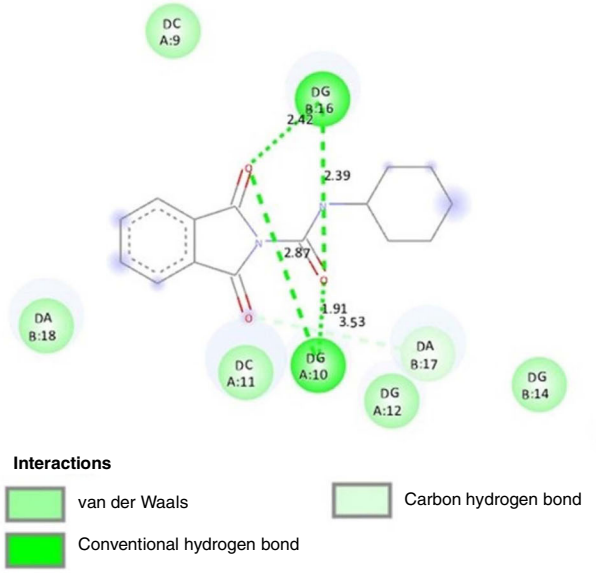
DC A:9
DG B:16
2.42
2.39
2.87
1.91
3.53
DA B:18
DC A:11
DG A:10
DA B:17
DG A:12
DG B:14
Interactions
van der Waals
Carbon hydrogen bond
Conventional hydrogen bond

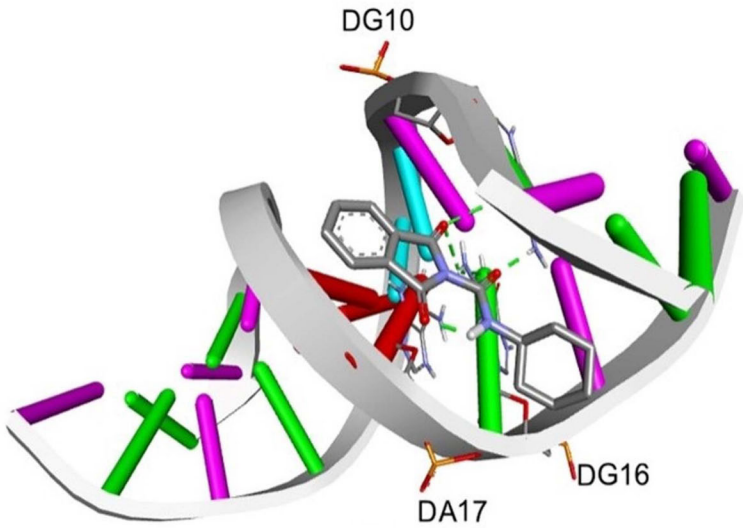
DG10
DG16
DA17

(**4e**)

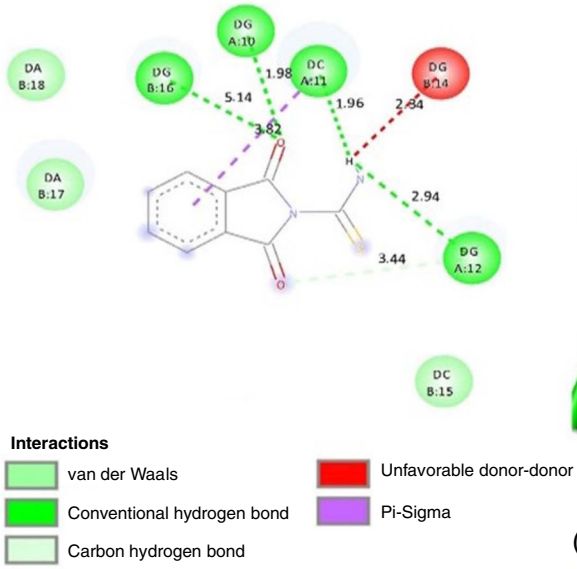
DG A:10
DA B:18
DG B:16
DC A:11
DG B:14
1.98
5.14
1.96
2.84
3.82
DA B:17
2.94
3.44
DG A:12
DC B:15
Interactions
van der Waals
Conventional hydrogen bond
Carbon hydrogen bond
Unfavorable donor-donor
Pi-Sigma

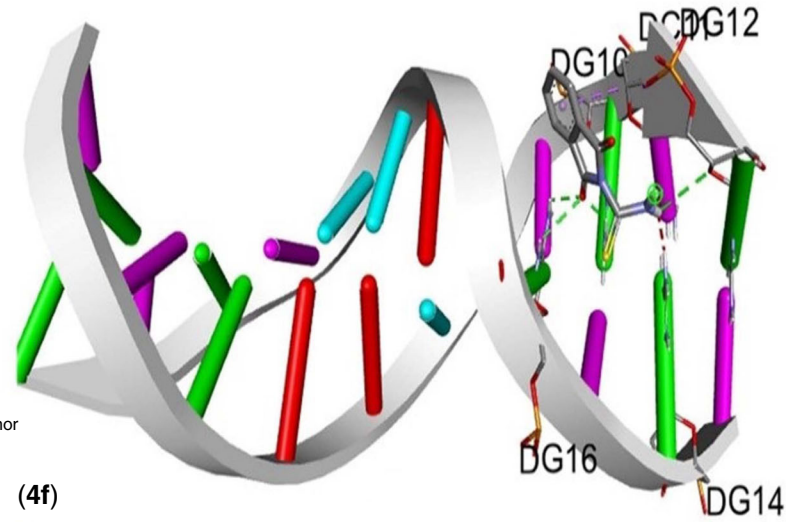
DG12
DG10
DG16
DG14

(**4f**)

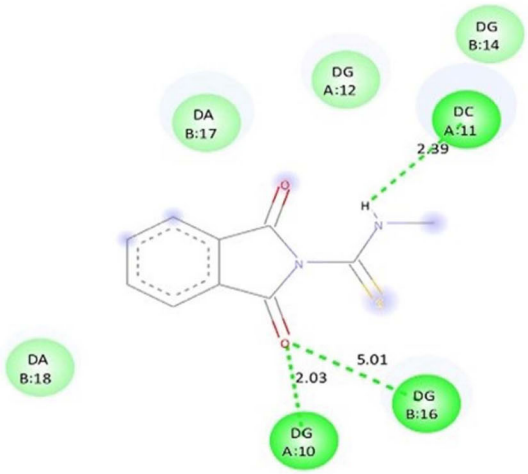
DG B:14
DG A:12
DA B:17
DC A:11
2.39
5.01
2.03
DA B:18
DG B:16
DG A:10
Interactions
van der Waals
Conventional hydrogen bond

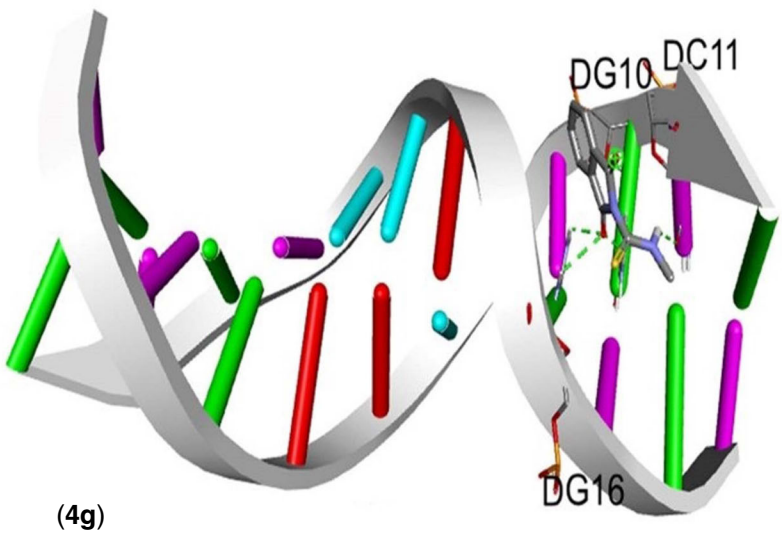
DG10
DC11
DG16

(**4g**)

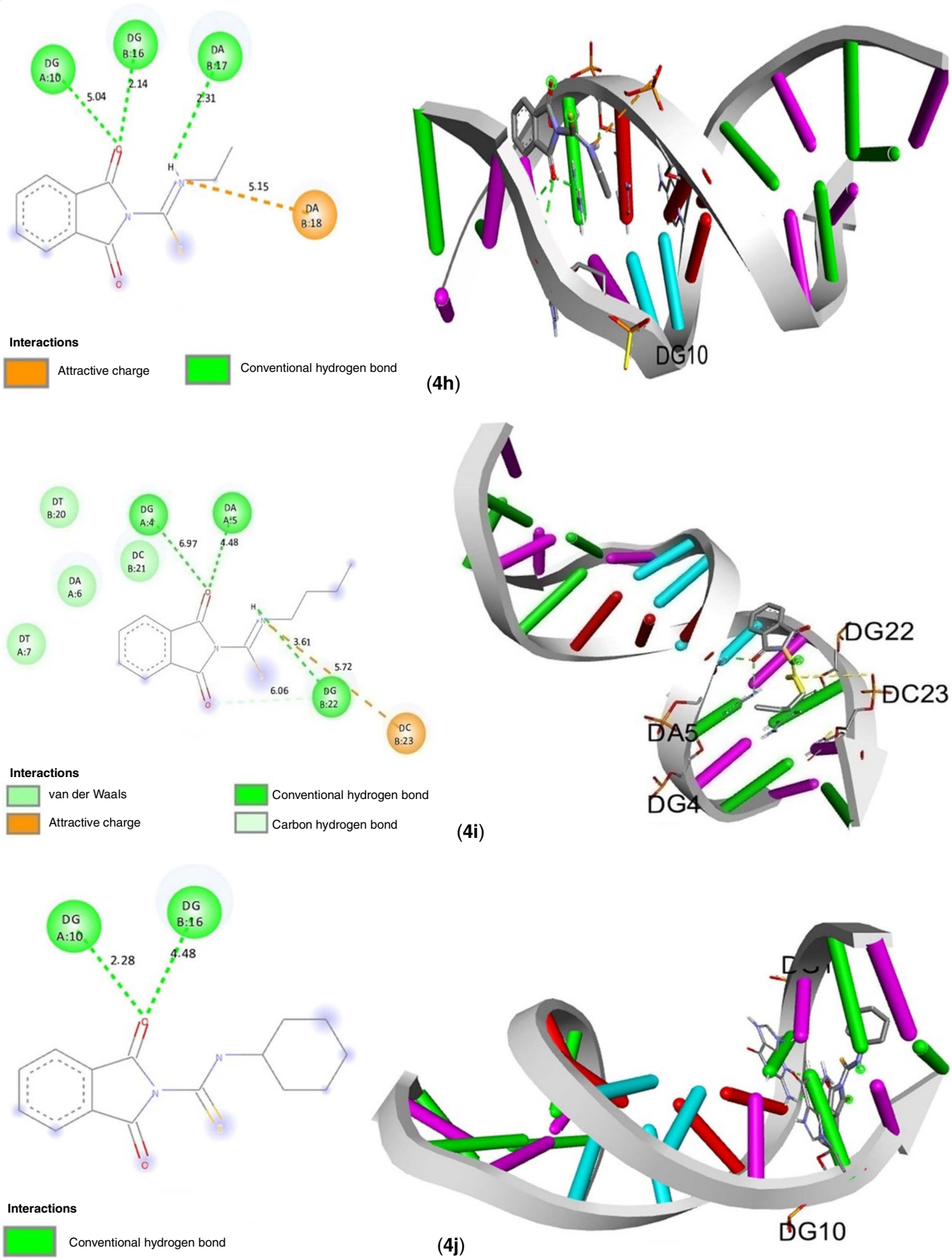

Fig. 2. Molecular docked 2D and 3D interaction diagram of **4a-j** with receptor 1bna from B-DNA

Pharmacokinetics and drug likeliness: The effectiveness of a drug is affirmed when it reaches its target in appropriate concentration and stays in the body in its bioactive form long enough. Drug likeliness of any molecule is ascertained by pharmacological descriptors such as molecular weight, lipophilicity, hydrogen bond donor and acceptor, topological polar surface area (TPSA) and water solubility [37]. The significantly lower TPSA values of synthesized compounds revealed their optimum permeability. Drug likeliness of an examined molecule is most reliably accessed by Lipinski rule of five [38], which is based on an acceptable range of different molecular descriptors such as molecular weight, TPSA, no of H-bond donor and acceptor and lipophilicity of drug molecules where a maximum of one violation is allowed. All the synthesized compounds follow Lipinski's rule of five with no violation, which reflects their satisfactory drug likeliness as compiled in Table-5.

TABLE-5
PHYSICO-CHEMICAL PROPERTIES RELATED TO LIPINSKI RULE OF 5 FOR THE SYNTHESIZED COMPOUNDS (**4a-j**)

Entry	MW (g/mol)	mLogP	No. of H-bond acceptor	No. of H-bond donor	nViol
Optimum range	≤ 500	≤ 5	≤ 10	≤ 5	≤ 1
4a	190.16	0.62	3	1	0
4b	204.18	0.92	3	1	0
4c	218.21	1.21	3	1	0
4d	246.26	1.76	3	1	0
4e	272.30	2.28	3	1	0
4f	206.22	0.63	2	1	0
4g	220.25	0.94	2	1	0
4h	234.27	1.23	2	1	0
4i	262.33	1.78	2	1	0
4j	288.36	2.30	2	1	0

Another important set of pharmacokinetic parameters [39], which plays a crucial role in *in silico* investigation of the compounds are shown in Table-6. Gastrointestinal (GI) absorption is related to the passage of a drug candidate in the bloodstream after administration. In present study, it is found that all the compounds possess high GI permeation and thus reach quickly and efficiently to the target sites. Regarding BBB permeation, all compounds are safer drug candidates except compounds **4d** and **4e**, which can pass through blood-brain barrier. P-glycoproteins shield our body from harmful chemicals by its efflux metabolism and all the compounds are non-substrate of the glycoprotein, which enhances their oral bioavailability. The different isoforms of cytochromes, namely CYP1A2, CYP2C19, CYP2C9, CYP2D6 and CYP3A4 play an essential role in deciding the efficacy of an administered drug by controlling its metabolism within the body. Most of the synthesized drug candidates illustrate minor inhibitory tendency towards different isoforms of cytochromes except CYP1A2. A negative skin permeability (log Kp) of the examined compounds signifies their low skin permeant ability.

Bioavailability radar is another effective tool based on the optimum range of six selected pharmacokinetic parameters

TABLE-6
PHARMACOKINETICS PARAMETER RELATED TO ADME FOR THE SYNTHESIZED COMPOUNDS (**4a-j**)

Compd.	GI absorption	BBB permeation	P-gp substrate	CYP1A2 inhibitor	CYP2C19 inhibitor	CYP2C9 inhibitor	CYP2D6 inhibitor	CYP3A4 inhibitor	Skin permeation (cm/s)	Bioavailability score
4a	High	No	No	No	No	No	No	No	-6.70	0.55
4b	High	No	No	Yes	No	No	No	No	-6.50	0.55
4c	High	No	No	Yes	No	No	No	No	-6.32	0.55
4d	High	Yes	No	Yes	No	No	No	No	-6.16	0.55
4e	High	Yes	No	Yes	No	No	No	No	-6.31	0.55
4f	High	No	No	Yes	No	No	No	No	-6.37	0.55
4g	High	No	No	Yes	No	No	No	No	-6.17	0.55
4h	High	No	No	Yes	No	No	No	No	-6.00	0.55
4i	High	No	No	Yes	Yes	Yes	No	No	-5.83	0.55
4j	High	No	No	Yes	Yes	Yes	No	No	-5.99	0.55

TABLE-7
PHYSICO-CHEMICAL PROPERTIES OF BIOAVAILABILITY RADAR FOR THE SYNTHESIZED COMPOUNDS (**4a-j**)

Compd.	MW (g/mol)	XlogP3	TPSA (Å^2)	Log S (ESOL)	Fraction of sp^3 carbon	No. of rotatable bonds
Optimum range	150 to 500	-0.7 to 5.0	20-130	-6 to 0	0.25 to 1	0 to 9
4a	190.16	1.07	80.47	-1.94	0.00	1
4b	204.18	1.47	66.48	-2.20	0.10	2
4c	218.21	1.84	66.48	-2.43	0.18	3
4d	246.26	2.31	66.48	-2.74	0.31	5
4e	272.30	2.32	66.48	-3.01	0.40	3
4f	206.22	1.67	95.49	-2.42	0.00	1
4g	220.25	2.07	81.50	-2.67	0.10	2
4h	234.27	2.44	81.50	-2.91	0.18	3
4i	262.33	2.91	81.50	-3.22	0.31	5
4j	288.36	2.92	81.50	-3.49	0.40	3

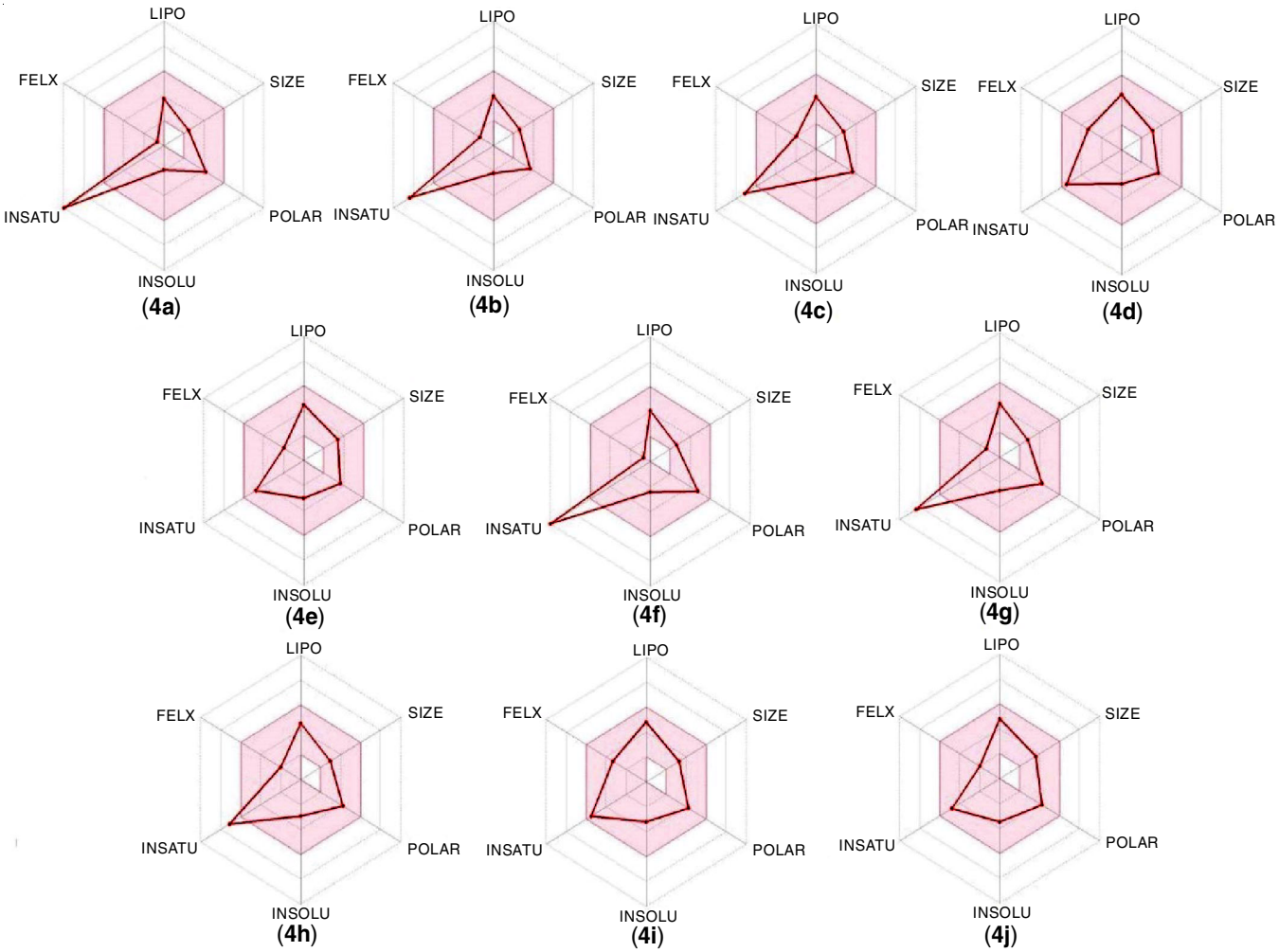

Fig. 3. Bioavailability radar for synthesized compounds (**4a-j**)

creating a pink radar region and any potential drug candidate within the pink region is declared to possess excellent oral bioavailability. All the examined compounds have good to excellent oral bioavailability based on compiled data in Table-7 and Fig. 3. The results of skin permeability and bioavailability radar favour the oral administration of the synthesized phthalimide derivatives compared to transdermal administration.

Pharmacokinetics and toxicity: The toxicity results obtained from the Osiris platform are compiled in Table-8, indicating **4a**, **4b**, **4c**, **4e**, **4f**, **4g** and **4j** as safe compounds with no risk alerts, while other shows orange and red alerts for specific toxicity risks.

TABLE-8
TOXICITY RISKS ASSESSMENT FOR THE SYNTHESIZED COMPOUNDS (**4a-j**)

Compd.	Mutagenic	Tumerogenic	Irritant	Reproductive effect
4a	Green	Green	Green	Green
4b	Green	Green	Green	Green
4c	Green	Green	Green	Green
4d	Orange	Green	Green	Green
4e	Green	Green	Green	Green
4f	Green	Green	Green	Green
4g	Green	Green	Green	Green
4h	Red	Red	Green	Orange
4i	Orange	Green	Green	Green
4j	Green	Green	Green	Green

Conclusion

In summary, a series of biologically active carboxamide and carbothioamide analogs of phthalimide have been efficiently synthesized under environmentally affable conditions. The direct one-step condensation of potassium phthalimide with (thio)ureas and use of water as a readily available and safe solvent media are noteworthy features of this protocol. The remarkable antioxidant potency and significant antibacterial efficacy of title compounds advocate their future application as therapeutics. The promising DNA binding propensity and the predicted ADMET profile of title compounds revealed their competencies as potential drug candidates.

ACKNOWLEDGEMENTS

The authors are thankful to Maharshi Dayanand University, Rohtak, India, for providing the necessary research facilities and support. Two authors, J.R. and R.G. thank CSIR and UGC, New Delhi, respectively, for providing the financial support.

CONFLICT OF INTEREST

The authors declare that there is no conflict of interests regarding the publication of this article.

REFERENCES

1. M.L. Almeida, M.C.V.A. Oliveira, I.R. Pitta and M.G.R. Pitta, *Curr. Org. Synth.*, **17**, 252 (2020); https://doi.org/10.2174/1570179417666200325124712
2. N. Kushwaha and D. Kaushik, *J. Appl. Pharm. Sci.*, **6**, 159 (2016); https://doi.org/10.7324/JAPS.2016.60330
3. A.M. Alanazi, A.S. El-Azab, I.A. Al-Suwaidan, K.E.H. ElTahir, Y.A. Asiri, N.I. Abdel-Aziz and A.A.-M. Abdel-Aziz, *Eur. J. Med. Chem.*, **92**, 115 (2015); https://doi.org/10.1016/j.ejmech.2014.12.039
4. S. Belluti, G. Orteca, V. Semeghini, G. Rigillo, F. Parenti, E. Ferrari and C. Imbriano, *Int. J. Mol. Sci.*, **20**, 28 (2019); https://doi.org/10.3390/ijms20010028
5. P.F. Lamie, J.N. Philoppes, A.O. El-Gendy, L. Rarova and J. Gruz, *Molecules*, **20**, 16620 (2015); https://doi.org/10.3390/molecules200916620
6. A. Davood, M. Iman, H. Pouriaiee, H. Shafaroodi, S. Akhbari, L. Azimidoost, E. Imani and S. Rahmatpour, *Iran. J. Basic Med. Sci.*, **20**, 430 (2017); http://doi.org/10.22038/IJBMS.2017.8586
7. I.M.M. Othman, M.A.M. Gad-Elkareem, M. El-Naggar, E.S. Nossier and A.E.-G.E. Amr, *J. Enzyme Inhib. Med. Chem.*, **34**, 1259 (2019); http://doi.org/10.1080/14756366.2019.1637861
8. H. Akgün, I. Karamelekoðlu, B. Berk, I. Kurnaz, G. Saribiyik, S. Oktem and T. Kocagöz, *Bioorg. Med. Chem.*, **20**, 4149 (2012); https://doi.org/10.1016/j.bmc.2012.04.060
9. A.A.-M. Abdel-Aziz, A.S. El-Azab, S.M. Attia, A.M. Al-Obaid, M.A. Al-Omar and H.I. El-Subbagh, *Eur. J. Med. Chem.*, **46**, 4324 (2011); https://doi.org/10.1016/j.ejmech.2011.07.002
10. C.Y. Okada-Junior, G.C. Monteiro, A.C.C. Aguiar, V.S. Batista, J.O. de Souza, G.E. Souza, R.V. Bueno, G. Oliva, N.M. Nascimento-Júnior, R.V.C. Guido and V.S. Bolzani, *ACS Omega*, **3**, 9424 (2018); https://doi.org/10.1021/acsomega.8b01062
11. S. Nagarajan, S. Majumder, U. Sharma, S. Rajendran, N. Kumar, S. Chatterjee and B. Singh, *Bioorg. Med. Chem. Lett.*, **23**, 287 (2013); https://doi.org/10.1016/j.bmcl.2012.10.106
12. W. Si, T. Zhang, L. Zhang, X. Mei, M. Dong, K. Zhang and J. Ning, *Bioorg. Med. Chem. Lett.*, **26**, 2380 (2016); https://doi.org/10.1016/j.bmcl.2015.07.052
13. R. Ronchetti, G. Moroni, A. Carotti, A. Gioiello and E. Camaioni, *RSC Med. Chem.*, **12**, 1046 (2021); https://doi.org/10.1039/D1MD00058F
14. R. Singh and K. Jakhar, *Der Pharma Chem.*, **8**, 175 (2016).
15. R.K. Mohapatra, P.K. Das, M.K. Pradhan, M.M. El-Ajaily, D. Das, H.F. Salem, U. Mahanta, G. Badhei, P.K. Parhi, A.A. Maihub and M.K. -E-Zahan, *Comments Inorg. Chem.*, **39**, 127 (2019); https://doi.org/10.1080/02603594.2019.1594204
16. K.C. Gulipalli, P. Ravula, S. Bodige, S. Endoori, P.K.R. Cherukumalli, J.N.N.S. Chandra and N. Seelam, *Russ. J. Gen. Chem.*, **90**, 1336 (2020); https://doi.org/10.1134/S1070363220070221
17. S. Konduri, V. Pogaku, J. Prashanth, V. Siva Krishna, D. Sriram, S. Basavoju, J.N. Behera and K.P. Rao, *ChemistrySelect*, **6**, 3869 (2021); https://doi.org/10.1002/slct.202004724
18. M.G. Gündüz, S.B. Ugur, F. Güney, C. Özkul, V.S. Krishna, S. Kaya, D. Sriram and S.D. Dogan, *Bioorg. Chem.*, **102**, 104104 (2020); https://doi.org/10.1016/j.bioorg.2020.104104
19. H. Sudhamani, G.S. Prasad, C. Venkataramaiah, C.N. Raju and W. Rajendra, *J. Recept. Signal Transduct.*, **39**, 373 (2019); https://doi.org/10.1080/10799893.2019.1683864
20. H.M. Faidallah, M.M. Al-Mohammadi, K.A. Alamry and K.A. Khan, *J. Enzyme Inhib. Med. Chem.*, **31(sup1)**, 157 (2016); https://doi.org/10.1080/14756366.2016.1180594
21. N. Siddiqui, M.S. Alam and J.P. Stables, *Eur. J. Med. Chem.*, **46**, 2236 (2011); https://doi.org/10.1016/j.ejmech.2011.03.004
22. V.R. Katla, R. Syed, M. Golla, A. Shaik and N.R. Chamarthi, *J. Serb. Chem. Soc.*, **79**, 283 (2014); https://doi.org/10.2298/JSC120716095K
23. A.A. Abdelhamid, A.M.M. Elsaghiera, S.A. Aref, M.A. Gad, N.A. Ahmed and S.A.A. Abdel-Raheem, *Curr. Chem. Lett.*, **10**, 371 (2021); https://doi.org/10.5267/j.ccl.2021.6.001
24. R.A.W.N. Filho, M.A.T. Palm-Forster and R.N. de Oliveira, *Synth. Commun.*, **43**, 1571 (2013); https://doi.org/10.1080/00397911.2011.651677
25. T.M. Pyriadi and N.J. Alasli, *J. Polym. Sci. A Polym. Chem.*, **27**, 2491 (1989); https://doi.org/10.1002/pola.1989.080270801
26. A.D. Jangale and D.S. Dalal, *Synth. Commun.*, **47**, 2139 (2017); https://doi.org/10.1080/00397911.2017.1369544
27. J.D. Moseley and C.O. Kappe, *Green Chem.*, **13**, 794 (2011); https://doi.org/10.1039/c0gc00823k
28. R. Arif, P.S. Nayab, Akrema, M. Abid, U. Yadava and Rahisuddin, *J. Anal. Sci. Technol.*, **10**, 19 (2019); https://doi.org/10.1186/s40543-019-0177-1
29. M.D. Hanwell, D.E. Curtis, D.C. Lonie, T. Vandermeersch, E. Zurek and G.R. Hutchison, *J. Cheminform.*, **4**, 17 (2012); https://doi.org/10.1186/1758-2946-4-17
30. S.K. Saha, A. Hens, N.C. Murmu and P. Banerjee, *J. Mol. Liq.*, **215**, 486 (2016); https://doi.org/10.1016/j.molliq.2016.01.024
31. M. Elshikh, S. Ahmed, S. Funston, P. Dunlop, M. McGaw, R. Marchant and I.M. Banat, *Biotechnol. Lett.*, **38**, 1015 (2016); https://doi.org/10.1007/s10529-016-2079-2
32. D.H. Truong, D.H. Nguyen, N.T.A. Ta, A.V. Bui, T.H. Do and H.C. Nguyen, *J. Food Qual.*, **2019**, 8178294 (2019); https://doi.org/10.1155/2019/8178294
33. O. Trott and A.J. Olson, *J. Comput. Chem.*, **31**, 455 (2010); https://doi.org/10.1002/jcc.21334
34. BIOVIA Dassault Systèmes, Discovery Studio Modeling Environment, Release (2017), San Diego: Dassault Systemes, (2016).
35. A. Daina, O. Michielin and V. Zoete, *Sci. Rep.*, **7**, 42717 (2017); https://doi.org/10.1038/srep42717
36. R. Srivastava, *ACS Omega*, **6**, 24891 (2021); https://doi.org/10.1021/acsomega.1c03736
37. M. Rashid, *Bioorg. Chem.*, **96**, 103576 (2020); https://doi.org/10.1016/j.bioorg.2020.103576
38. C.A. Lipinski, F. Lombardo, B.W. Dominy and P.J. Feeney, *Adv. Drug Deliv. Rev.*, **23**, 3 (1997); https://doi.org/10.1016/S0169-409X(96)00423-1
39. J. Dharani and S. Ravi, *Asian J. Chem.*, **32**, 1421 (2020); https://doi.org/10.14233/ajchem.2020.22569